Biomaterials 51 (2015) 138–150

Contents lists available at ScienceDirect

Biomaterials

journal homepage: www.elsevier.com/locate/biomaterials

Functional maturation of human pluripotent stem cell derived cardiomyocytes *in vitro* – Correlation between contraction force and electrophysiology

Marcelo C. Ribeiro [a], Leon G. Tertoolen [a], Juan A. Guadix [a, b], Milena Bellin [a], Georgios Kosmidis [a], Cristina D'Aniello [a], Jantine Monshouwer-Kloots [a], Marie-Jose Goumans [c], Yu-li Wang [d], Adam W. Feinberg [d, e], Christine L. Mummery [a], Robert Passier [a, *]

[a] Department of Anatomy & Embryology, Leiden University Medical Center, Leiden, The Netherlands
[b] Department of Animal Biology, University of Málaga, Málaga, Spain
[c] Department of Molecular Cell Biology, Cancer Genomics Centre, Centre for Biomedical Genetics, Leiden University Medical Center, Leiden, The Netherlands
[d] Department of Biomedical Engineering, Carnegie Mellon University, Pittsburgh, PA, USA
[e] Department of Materials Science and Engineering, Carnegie Mellon University, Pittsburgh, PA, USA

ARTICLE INFO

Article history:
Received 6 November 2014
Accepted 25 January 2015
Available online

Keywords:
Human pluripotent stem cells
Human fetal cardiomyocytes
Cardiomyocyte maturation
Cardiomyocyte contraction force

ABSTRACT

Cardiomyocytes from human pluripotent stem cells (hPSC-CM) have many potential applications in disease modelling and drug target discovery but their phenotypic similarity to early fetal stages of cardiac development limits their applicability. In this study we compared contraction stresses of hPSC-CM to 2nd trimester human fetal derived cardiomyocytes (hFetal-CM) by imaging displacement of fluorescent beads by single contracting hPSC-CM, aligned by microcontact-printing on polyacrylamide gels. hPSC-CM showed distinctly lower contraction stress than cardiomyocytes isolated from hFetal-CM. To improve maturation of hPSC-CM *in vitro* we made use of commercial media optimized for cardiomyocyte maturation, which promoted significantly higher contraction stress in hPSC-compared with hFetal-CM. Accordingly, other features of cardiomyocyte maturation were observed, most strikingly increased upstroke velocities and action potential amplitudes, lower resting membrane potentials, improved sarcomeric organization and alterations in cardiac-specific gene expression. Performing contraction force and electrophysiology measurements on individual cardiomyocytes revealed strong correlations between an increase in contraction force and a rise of the upstroke velocity and action potential amplitude and with a decrease in the resting membrane potential.

We showed that under standard differentiation conditions hPSC-CM display lower contractile force than primary hFetal-CM and identified conditions under which a commercially available culture medium could induce molecular, morphological and functional maturation of hPSC-CM *in vitro*. These results are an important contribution for full implementation of hPSC-CM in cardiac disease modelling and drug discovery.

1. Introduction

The efficiency of cardiomyocyte differentiation of human pluripotent stem cells (hPSC) has greatly improved in recent years [1], with many reports describing more than 60% cardiomyocytes in differentiated cultures. For most laboratories, generating hPSC-derived cardiomyocytes (hPSC-CM) is no longer a major hurdle, providing opportunities for disease modelling, drug toxicity screening and identifying drug sensitivities of certain genotypes [2,3]. However, hPSC-CM are immature compared with human adult cardiomyocytes and express typical fetal cardiac genes [4], have immature electrophysiological properties such as low resting membrane potential and slow upstroke velocities [5], use glucose as major energy source as opposed to the fatty acids used by adult

* Corresponding author.
E-mail address: r.passier@lumc.nl (R. Passier).

http://dx.doi.org/10.1016/j.biomaterials.2015.01.067
0142-9612/

cardiomyocytes [6], have underdeveloped, (partially) disarrayed sarcomeres, heterogeneous shapes and are smaller in size [7,8]. Several studies have reported that the contraction stress of hPSC-CM using hydrogel-based technologies in two (2D) and three dimensions (3D) varied from 0.22 ± 0.70 mN/mm^2 to 11.8 ± 4.5 mN/mm^2 [9–12]. Furthermore, it has also been shown that contraction stress is dependent on substrate stiffness [13], emphasizing the necessity of using similar substrate stiffness for comparison of contraction stress values between different conditions.

Optimal implementation of hPSC-CM in human cardiac disease modelling and drug toxicity screening, would benefit from greater maturation of hPSC-CM. Therefore, it is important to understand which physiological parameters impact features of maturation. Candidate parameters that have been examined to date include long-term culture to mimic developmental gestation [14], substrate stiffness [15], cell patterning and alignment as occurs in the normal heart [16,17], electrical and mechanical stimulation [18], mechanical loading [19], interaction with other cell-types [20], and interference with signalling pathways thought to be of importance in heart development The outcomes of these studies have been variable: in assessing the effects of long-term culture, hPSC-CM were reported to withdraw from the cell-cycle and show ultrastructural maturation in 35 days [21] and increased conduction velocities in 2 months [22] but no improvements in contraction force were observed up to 2 or 3 months in culture [9,13] Following hPSC-CM for even longer, up to 4 months, both morphological and functional maturation were reported for both human embryonic stem cell (hESC) and human induced pluripotent stem cell (hiPS)-derived cardiomyocytes [14]. In assessing the role of substrate stiffness, neonatal rat ventricular myocytes (NRVM) cultured on a glass substrate (Young's Modulus ≈50 GPa), which is six orders of magnitude stiffer than heart tissue [23], showed decreased length to width ratios and increased stress fibre content compared to NRVM on substrates with Young's Modulus of 10 kPa [15,23]. Both stiffness and cell shape have regulatory roles in cytoskeletal architecture and extra cellular matrix (ECM) coupling [24]. In turn, the cytoskeletal architecture is known to regulate gene expression [25], impulse propagation [26], excitability [27] and contraction [16,28], demonstrating the regulatory role of cell shape on cardiac function. *In vivo,* adult ventricular cardiomyocytes are elongated and aligned along one axis with length/width ratios of 7:1 [17,24]. Accordingly, restraining cell shape to a more elongated phenotype reminiscent of that of adult cardiomyocytes improves cardiomyocyte structure and function [16,29]. Thyroid hormones also have an important influence on cardiac structure, electrophysiological functions and cardiac contractility in development *in vivo* [30], by directly regulating key structural and regulatory genes such as *α-MHC* and *β-MHC*, *SERCA2*, *PLN*, and various ion channels [31]. Moreover, triiodothyronine (T3) has been described as promoting electrophysiological and calcium handling maturation in mouse embryonic stem cell derived cardiomyocytes [32] and contraction maturation hiPS-CM [33].

Alterations in cardiomyocyte transcriptional, biochemical and functional cues, manifested by changes in electrophysiology, calcium handling, bioenergetics and contraction force, are inherent to progression from fetal to an adult state [8]. Consequently, *in vitro* cardiomyocyte maturation state can be assessed by analyses of these features. Nevertheless, the relationship and interdependence of these different parameters are poorly understood. Here, we found that hPSC-CM generate lower contraction stress than second trimester (16 week) human fetal cardiomyocytes (hFetal-CM) at the same substrate stiffness. Furthermore, by making use of different maturation media we were able to demonstrate that hPSC-CM displayed improved sarcomeric structure organization, stronger contraction stress, improved electrophysiological parameters and changes in gene expression compatible with a more developmentally advanced stage. Additionally, we assessed the relation between electrophysiology and contraction force during cardiomyocyte maturation by analysing these parameters on the same cardiomyocyte.

2. Materials and methods

A detailed description of experimental methods is provided in the Online data supplement.

2.1. hESC and hiPS cell maintenance and differentiation to cardiomyocytes

Both hESC and hiPS lines were cultured on irradiated mouse embryonic fibroblasts (MEFs). Differentiation to cardiomyocytes was as described previously [34]. Briefly, spin embryoid bodies (spinEB) were formed by centrifugation of cells into aggregates in a 96-well format (Greiner) with BSA polyvinylalcohol essential lipids medium (BPEL) [35] together with 35 ng/ml bone morphogenetic protein 4 (BMP4) (R&D), 30 ng/ml Activin A (Miltenyi), 30 ng/ml vascular endothelial cell growth factor (VEGF) (Miltenyi), 40 ng/ml stem cell factor (SCF) (Miltenyi), 1.5 μM CHIR99021 (Axon Medchem). The medium was refreshed on day 3 (Supplementary Fig. 1). SpinEBs started beating between day 7 and 10 of differentiation.

2.2. Culturing and plating of hPSC derived cardiomyocytes

Two commercially available media, Cardiomyocyte medium (CA) and Maturation medium (MM) (available as Pluricyte Medium from Pluriomics BV), were used in a stepwise manner to mature hPSC-CM *in vitro*. CA and MM (containing T3 hormone) are serum-free, defined, nutrient-rich media that were pre-optimized for viability in culture and morphological maturation of hPSC-CMs. Differentiated cardiomyocytes were dissociated at day 10 with 1× TryplE select (Gibco) for 10 min and plated as single cells in BPEL on 0.1% gelatin (Sigma)-coated 6-well plates in order to change from a spinEB to a monolayer culture format. This step is crucial for proper cell attachment to the gelatin lines later on. On day 13, the medium was changed to BPEL or CA (Supplementary Fig. 1). On day 20, one well of each condition was dissociated as described above and seeded on the polyacrylamide gel patterned with 1% gelatin lines, in the respective medium. The medium was refreshed the next day and contraction and electrophysiological characteristics measured three days after plating. In the remaining culture wells the medium was changed to BPEL, CA and MM on day 20 as described in Supplementary Fig. 1. The cells were cultured in the respective media for ten more days. As before, on day 30 the cells were dissociated with 10× Tryple select (Gibco) and seeded on the polyacrylamide gel patterned with 1% gelatin lines, in the respective medium. The cells were refreshed next day and contraction and electrophysiological characteristics measured three days after plating.

2.3. Human fetal cardiomyocyte isolation and culture

Human fetal hearts were collected after elective abortion following individual informed consent, after approval by the Medical Ethical Committee of Leiden University Medical Center. The investigation conforms to the principles outlined in the Declaration of Helsinki. The fetal heart was examined for any apparent anomalies before single cell isolation. The hearts were cut into small pieces and subsequently dissociated in collagenase A (Roche) Calcium-free Tyrode's buffer. To minimize the amount of fibroblasts, the cells were pre-plated on a 10 cm dish for 45 min. The remaining cells were plated directly on the polyacrylamide gel patterned with 1% gelatin lines and kept at 37 °C, 5%CO_2. The medium was refreshed next day and measurements were made three days after plating.

2.4. Patterned polyacrylamide gel fabrication

Patterned polyacrylamide gels were prepared as previously described [36]. Briefly, a polydimethylsiloxane (PDMS) stamp was incubated with 1% gelatin (Sigma) for 1 h. The stamp was used to μcontact-print a pattern of 20 μm wide gelatin lines with 20 μm spacing onto 15 mm coverslips. The polyacrylamide solution was prepared with a final concentration of 0.1% bis-acrylamide (Bio-Rad), 5% acrylamide (Bio-Rad) and 10 mM HEPES pH 8.5 in distilled water, followed by centrifugation for 1 min at 10.000RPM for degassing. 0.006% (m/v) of ammonium persulphate (Sigma–Aldrich) and a 1:1000 dilution of 0.2-μm fluorescent beads (Ex/Em: 660/680 nm - Molecular Probes) were added to the solution and briefly Vortexed. The gel polymerization was initiated with TEMED (Bio-Rad) and 9.2 μl of the final solution was added to a 25 mm coverslip treated with plus Bind-Silane solution (GE Healthcare). The μcontact-printed 15 mm coverslip was placed on top of the drop with the gelatin lines facing the gel. After 20 min of polymerization, the 15 mm coverslip was removed and a 25 mm coverslip was mounted onto a well of a glass bottomed 6-well plate (Mattek), replacing the initial glass. The polymerized gel has a Young's modulus of 5.8 kPa [37].

2.5. Contraction force measurements

The contraction force measurements were performed as previously described [13]. Briefly, using a Leica AF-6000LX microscope with controlled temperature and

CO_2, 40× image series of brightfield and fluorescent beads were taken at 5 frames per second of aligned single self-pacing cardiomyocytes. Single frames from maximal relaxation and contraction of the brightfield and fluorescent image series were analyzed by the LIBTRC software package (kindly provided by Dr. Micah Dembo), creating a mask of the cell outline from the brightfield image and a vector map from the difference between the relaxed and contracted fluorescent images. The vector map and the cell mask were used to calculate the total force that the cell applies on the substrate at its maximum peak of contraction. The contraction stress generated by the cardiomyocyte was calculated by dividing the total force by the cell surface area.

2.6. Electrophysiology

After contraction force measurements, the position of each cell was noted by its quadrant localization and by 10× and 40× brightfield images. Subsequently, the coverslips were transferred to the patch-clamp electrophysiology set up. Measurements were performed with the amphothericin-perforated patch-clamp technique using the Axopatch 200B patch clamp amplifier (Molecular Devices Axon Instruments, U.S.A.) at 5 kHz in the fast current clamp mode.

2.7. Gene expression analysis

Cardiomyocytes derived from the HES3-NKX2-5-eGFP line [34] were cultured in the different test media (Supplementary Fig. 1) and purified by sorting on day 20 and 30 of differentiation. RNA from day 20 and 30 cells was isolated using the RNeasy-MicroKit (Qiagen) and Nucleo Spin RNA XS (Macherey-Nagel), respectively, and reverse transcribed to cDNA using the Iscript cDNA (BioRad). Gene expression analysis was performed by q-PCR using IQ SYBR Green (BioRad). The samples were normalized to the house keeping gene human Acidic Ribosomal Protein (*RPLP*). The primers used can be found in supplementary Table 1.

2.8. Immunocytochemistry and sarcomere structure evaluation

After contraction measurements, the cells were fixed on the lines with 4% paraformaldehyde. For identification of sarcomeres and cell boundaries the samples were incubated with the primary antibodies mouse anti α-actinin (Sigma–Aldrich A7811) and rabbit anti pan-cadherin (Sigma–Aldrich C3678) followed by the secondary antibodies donkey anti mouse IgG Cy3 (Jackson ImmunoResearch Europe 715-165-150) and donkey anti rabbit IgG A488 (Santa Cruz Biotechnology sc-15368). The sarcomeric structure of individual cardiomyocytes was determined by grading the organization of α-actinin into four different classes of individual aligned cells at 40× using the AF-6000 Leica microscope [38]. Sarcomere profiles were constructed with the function *Plot Profile* of ImageJ (http://imagej.nih.gov). Software developed in house (LabVIEW, National Instruments Corporation, Austin, U.S.A.) was used to analyze the average spacing distance by the method of power spectral analysis applied to the profile data from ImageJ (μm/pixel).

2.9. Statistical analysis

Differences between the different groups were assessed by Student's t-test for comparison of two groups or one-way ANOVA followed by Bonferroni post-test for comparison of three or more groups. The differences in cell structure classification were assessed using Chi^2 test. Significance was attributed to comparisons with values of $P < 0.05^*$; $P < 0.01^{**}$; $P < 0.001^{***}$. All error bars represent SEM.

3. Results

3.1. Contraction stresses of hESC-CM and hiPS-CM are comparable

hESC-CM and hiPS-CM (hPSC-CM) were routinely differentiated and maintained in BPEL medium then dissociated on day 10 and plated on 0.1% gelatin (Supplementary Fig. 1). To analyze cardiomyocyte function in physiologically relevant substrate dimensions and stiffness specifically, hPSC-CM were dissociated on differentiation day 20 and seeded on 20 μm wide 1% gelatin lines that were μcontact-printed on polyacrylamide gel (Fig. 1A). Three days after seeding, measurements of contraction force by

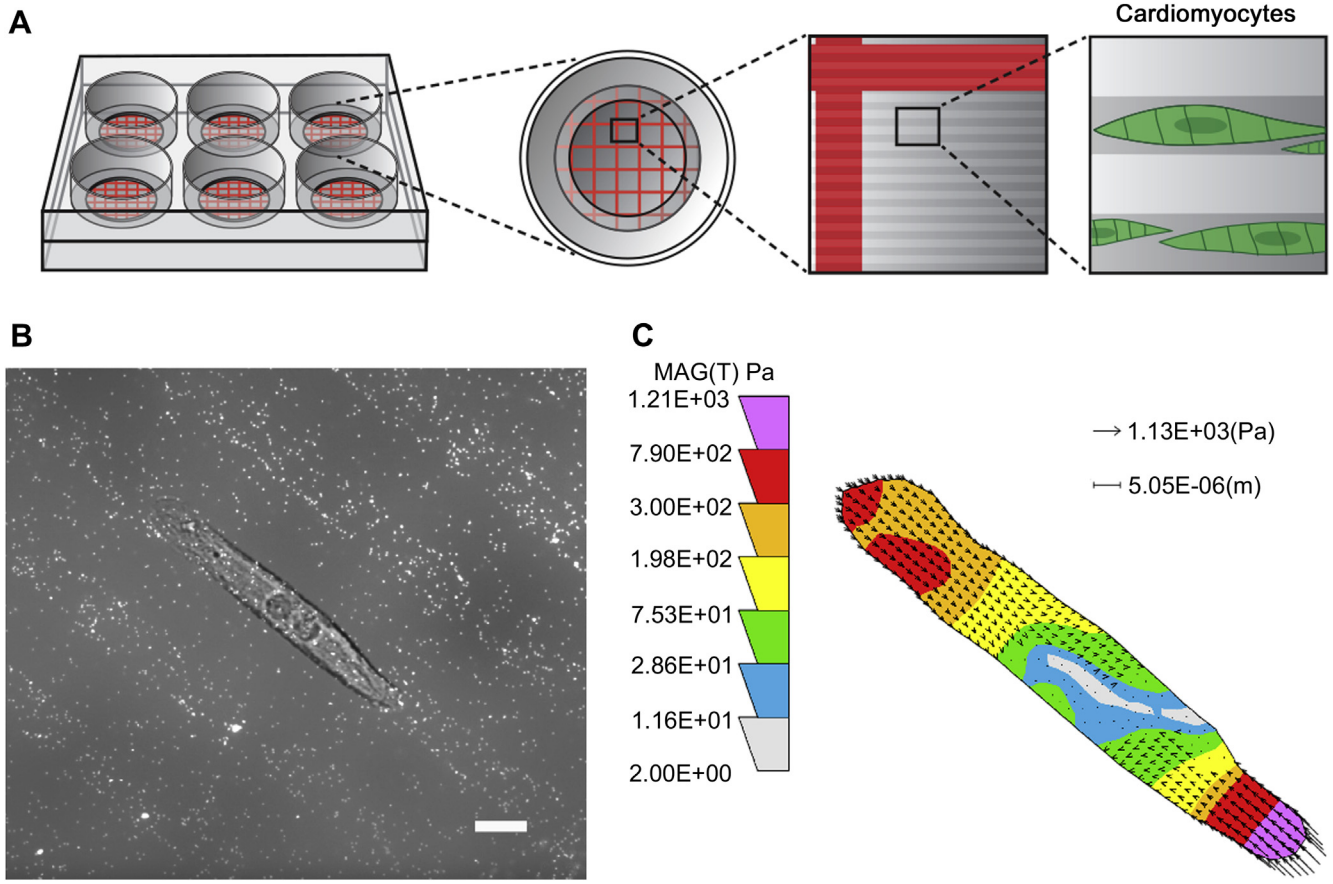

Fig. 1. Schematic overview of measuring traction stress. A. A bottomless 6-well plate with the 25 mm coverslips carrying the polyacrylamide gel with patterned gelatin (darker gray lines) and red quadrant grid. **B**. Merge of the bright field image of a single cardiomyocyte with the fluorescent image of the fluorescent beads embedded in the gel, representing the image acquisition during measurements. Scale bar 10 μm. **C**. Heat map generated by the LIBTRC software representative of the traction stress applied by the cell on the substrate ($1Pa = 10^{-3}$ mN/mm^2). (For interpretation of the references to colour in this figure legend, the reader is referred to the web version of this article.)

spontaneously beating cardiomyocytes were performed by imaging displacement of fluorescent beads embedded in the gels (Fig. 1B). From the contraction cycle, frames corresponding to maximal contraction and relaxation of single cardiomyocytes were compared and analyzed using LIBTRC traction force microscopy software, creating a vector heat-map with the total force produced by each cell at the peak of contraction (Fig. 1C). To compensate for variation in contraction force (nN) induced by differences in cell size, total force was normalized to cell surface area (μm^2) and designated as contraction stress (mN/mm^2). First, we determined contraction stresses of hESC-CM and hiPS-CM under standard differentiation culture conditions (BPEL) on day 23. The contraction stress generated by hESC-CM and hiPS-CM were comparable (0.29 ± 0.01 mN/mm^2 and 0.26 ± 0.01 mN/mm^2, respectively; $P = 0.17$) (Fig. 2A). In accordance, cardiomyocyte morphology and sarcomeric organization were similar on micropatterned lines, demonstrated by expression and localization of sarcomeric protein α-actinin (Fig. 2B). In accordance with contraction stress, hESC-CM and hiPS-CM have similar cell surface area (hESC-CM 1050 ± 55.01 μm^2 versus hiPS-CM 1244 ± 49.92 μm^2 $P = 0.055$) (supplementary Fig. 3).

3.2. hPSC-CMs generate less contraction stress than hFetal-CM

Since previous studies have reported that hPSC-CM resemble hFetal-CM based on gene expression [4], electrophysiology [5] and morphology [39] we assessed the degree of contraction maturity in relation to fetal developmental stage by comparing hPSC-CM to cardiomyocytes from second trimester human embryos. As reported previously, contraction stress generated by a single cardiomyocyte is intrinsically dependent on the stiffness of the substrate [13]. Therefore contraction stresses of all cardiomyocytes were determined on the same substrate. hFetal-CM isolated from hearts of 14 (N = 1), 17 (N = 2) and 19 (N = 1) weeks of gestation fetuses were seeded onto 1% gelatin lines microcontact-printed on polyacrylamide gels and cultured for three days before contraction force measurements. Cardiomyocyte populations from all four human fetal hearts generated similar contraction stresses (14 weeks 0.42 ± 0.04 mN/mm^2; 17 weeks 0.42 ± 0.03 mN/mm^2; 19 weeks 0.39 ± 0.02 mN/mm^2 $P = 0.78$) (Fig. 2A), indicating unchanged contraction stress levels of cardiomyocytes over this gestational period. However, in hESC-CM and hiPS-CM, contraction stresses were significantly lower than hFetal-CM (Fig. 2A). Correspondingly, α-actinin staining demonstrated greater sarcomeric organization (Figs. 2B and 4B) in hFetal-CM than in hPSC-CMs. The cell surface areas of hFetal-CM were similar (1216 ± 44.60 μm^2) to the hPSC-CM population ($P = 0.055$) (Supplementary Fig. 3).

3.3. Improvement of hPSC-CM function in vitro

In order to improve contractile force in hPSC-CM, we introduced a step-wise change in culture conditions of the cardiomyocytes. We first changed the culture format from aggregates to monolayer on day 10. Three days after plating, the medium was changed to CA. After incubation of hESC-CM and hiPS-CM in CA for ten days (from day 13–23 - Supplementary Fig. 1) contraction stress increased by 51% and 66%, respectively, compared to cardiomyocytes maintained in standard differentiation medium BPEL (hESC-CM in CA 0.43 ± 0.03 mN/mm^2 $P < 0.0001$ and hiPS-CM in CA 0.43 ± 0.02 mN/mm^2 $P < 0.0001$) (Fig. 3A). Interestingly, the contraction stress generated by hPSC-CM maintained in CA reached similar levels to that in second trimester hFetal-CM ($P = 0.6417$) (Fig. 3A), indicating

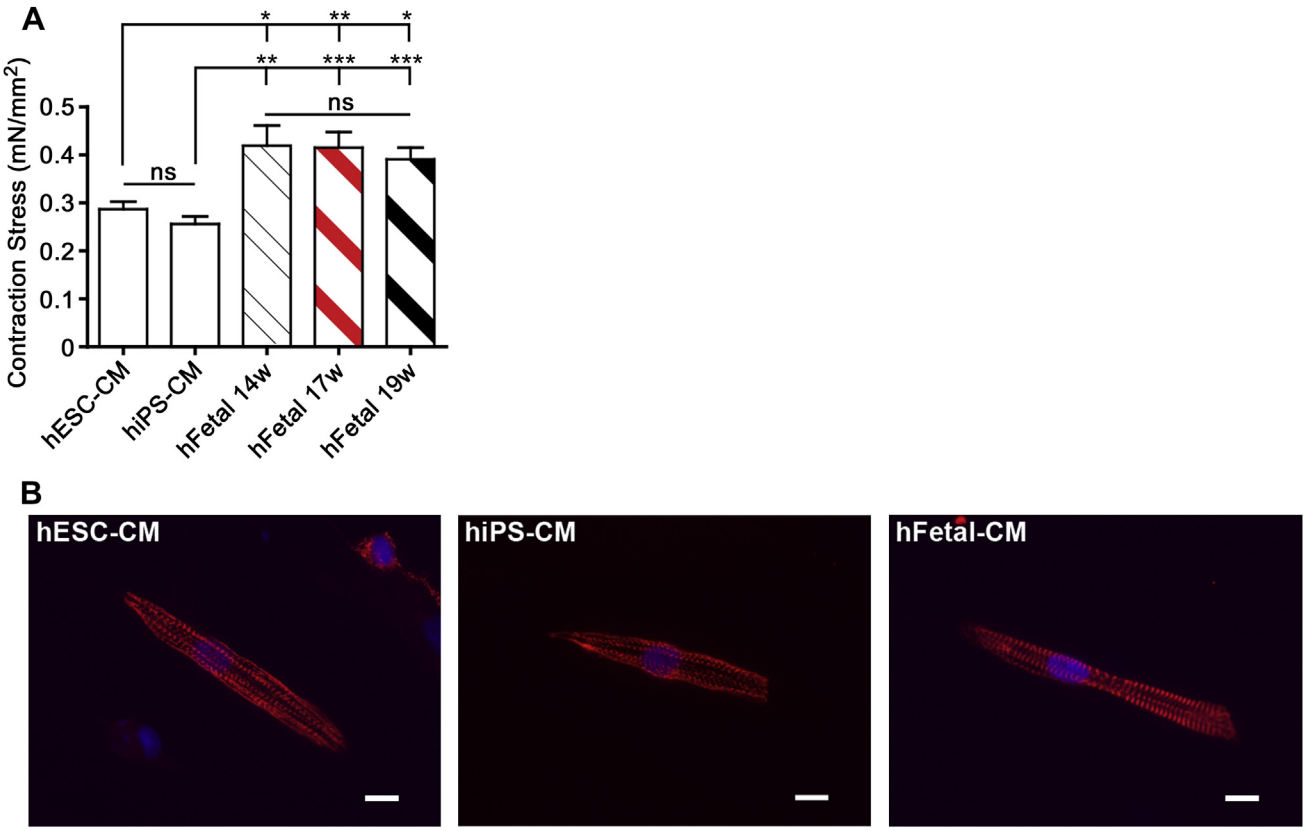

Fig. 2. Comparison of contraction stresses between hPSC-CM and 2nd trimester hFetal-CM. A. Mean contraction stress generated by hESC-CM (n = 45), hiPS-CM (n = 45) and 14 week hFetal-CM (1 heart; n = 16), 17 week hFetal-CM (average of 2 hearts; n = 50) and 19 week hFetal-CM (1 heart; n = 50). ns = non-significant; *P < 0.05; **P < 0.01; ***P < 0.001. **B.** Representative images of α-actinin staining of hESC-CM, hiPS-CM and hFetal-CM. Scale bar 10 μm.

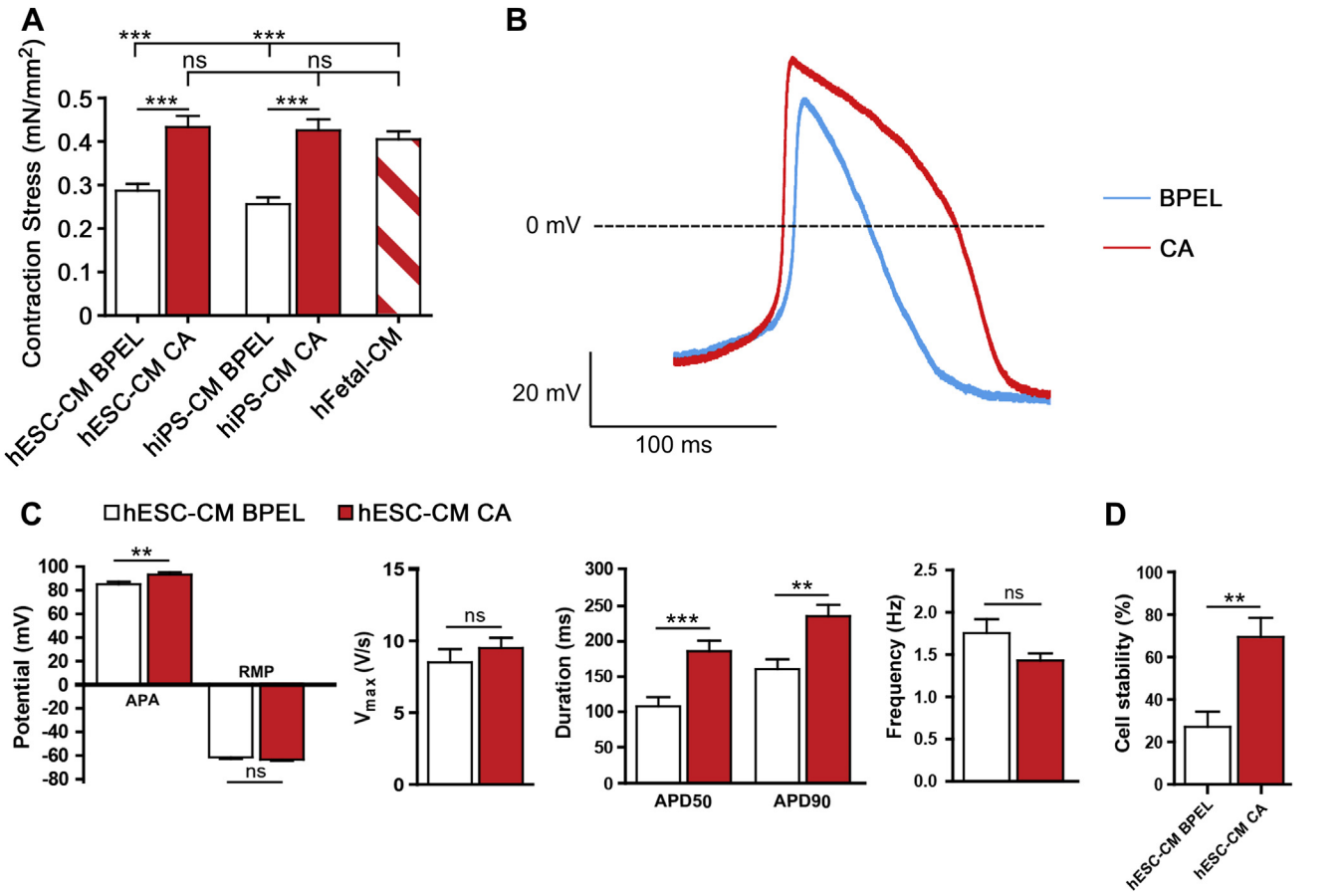

Fig. 3. Functional improvement of hPSC-CM *in vitro*. A. Mean contraction stress at day 23 generated by hESC-CM in BPEL (n = 45) and CA (n = 41) and hiPS-CM in BPEL (n = 45) and CA (n = 43) and in hFetal-CM combined (mean of 4 hearts between week 14 and 19; n = 116). **B.** Representative examples of spontaneous AP of hESC-CM in the two different media. **C.** Electrophysiological comparison between hESC-CM in BPEL (n = 18) and in CA (n = 24), with APA, APD50 and APD90, RMP, Vmax, and beating frequency. **D.** Percentage of stable hESC-CM in CA when compared to BPEL. ns = non-significant; **P < 0.01; ***P < 0.001.

progressive contractile maturation. Furthermore, the hPSC-CM population almost doubled in surface area in CA (hESC-CM in CA 2067 ± 169.2 μm^2 $P < 0.0001$ and hiPS-CM in CA 1866 ± 98.85 μm^2 $P < 0.0001$) (Supplementary Fig. 3). Since contraction stresses of both hESC-CM and hiPS-CM populations in CA were similar, further functional analyses were performed on hESC-CM only. Since we used the hESC-NKX2-5-eGFP cardiac reporter line [34] we could sort single cardiomyocytes based on GFP expression.

In addition to contraction stress, electrophysiological analysis is an important functional readout for assessing maturity of cardiomyocytes [5]. Electrophysiological measurements were performed by patch-clamp on single hESC-CM previously maintained in control (BPEL) or in CA media. In order to compare changes in electrophysiological parameters with changes in contraction force, both assays were performed on the same cell. Contraction force was first determined in 15–20 cardiomyocytes per coverslip in control (BPEL) and CA, followed by electrophysiological measurements in Tyrode's solution. Action potential duration (APD) was significantly prolonged at 50% (APD50) and 90% (APD90) repolarization in CA, in both spontaneously beating and paced cardiomyocytes at all tested frequencies (1, 2, 3 Hz). Furthermore action potential amplitude (APA) was increased in spontaneously beating and 2 Hz-paced cardiomyocytes, indicating more mature action potential (AP) shapes (Fig. 3B and C Supplementary Table 2). Nevertheless, no differences on the upstroke velocity (Vmax) or resting membrane potential (RMP), important parameters reflecting cardiomyocyte maturity, were observed (Fig. 3C; Supplementary Table 2). Besides the differences in contraction stress and electrophysiological measurements of hESC-CM cultured in BPEL or CA, there was also a clear difference in the "stability" of cardiomyocytes. Switching medium from that used for contraction force measurements to Tyrode's solution used for electrophysiology frequently resulted in a contractile arrest without measurable action potentials during patch-clamp. From hESC-CM cultured in BPEL only 25% (21 of 84) had measurable APs, while from the same population cultured in CA 65.9% (29 of 44) of the hESC-CM had measurable APs (Fig. 3D), suggesting increased single cell stability *in vitro*.

To investigate a possible relationship between functional changes in contraction stress and electrophysiology and changes in gene expression, RNA from GFP/Nkx2.5 sorted hESC-CM cultured in BPEL and CA was isolated and quantified by q-PCR. Expression of cardiac genes showed no differences between groups (Fig. 4A). To determine the level of morphological maturation, sarcomeric organization was analyzed. Sarcomeres in aligned hPSC-CM were immunostained for α-actinin and the sarcomere pattern in each cell was graded into four different classes [38]: Class I cells display a random or patterned dotted staining; Class II cells display parallel bands in less than 70% of the cell; Class III display parallel band patterned staining in more than 70% and less than 90% of the cell; Class IV display high sarcomeric organization with parallel bands in more than 90% of the cell (Supplementary Fig. 2). Both hESC-CM and hiPS-CM in CA displayed significant increases in sarcomeric organization relative to BPEL with a shift from class I to II (Fig. 4B and C). Moreover, both cardiomyocyte populations displayed

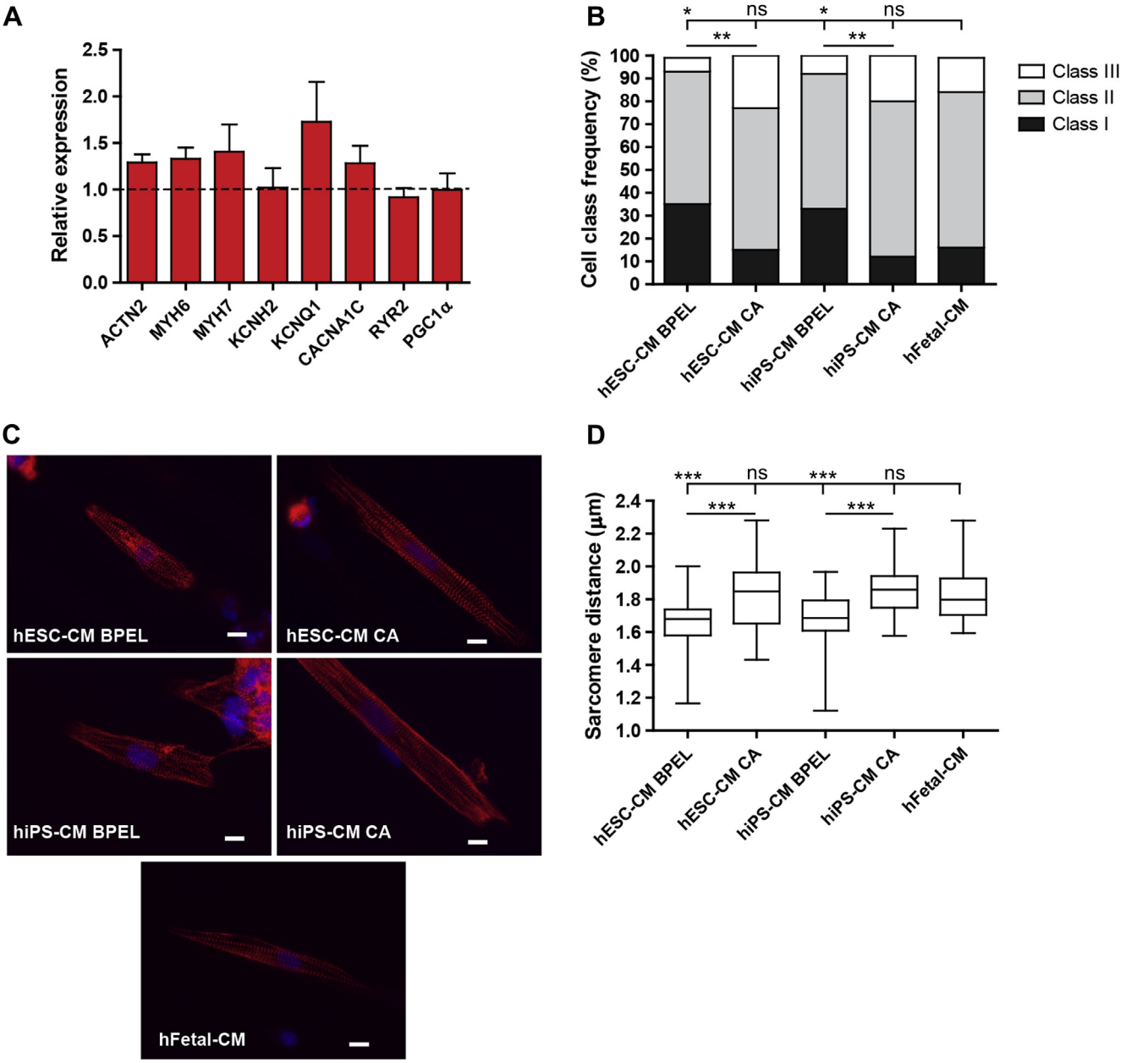

Fig. 4. Characterization of gene expression and sarcomeric organization of hPSC-CM. **A**. Relative gene expression of cardiac genes by for hESC-CM in CA at day 23 compared to expression levels of these genes in hESC-CM in BPEL (dotted line). Expression levels were normalized to *RPLP* expression. **B**. Classification of sarcomeric organization of hFetal-CM (n = 76) and hESC-CM and hiPS-CM in BPEL (n = 77 and n = 75, respectively) and CA (n = 74 for both). **C**. Representative images of α-actinin staining (red) and nuclei (blue) of hESC-CM, hiPS-CM in BPEL and in CA, and of hFetal-CM. Scale bar 10 μm. **D**. Median, maximum and minimum sarcomere lengths of hESC-CM and hiPS-CM in BPEL (n = 53 and n = 58, respectively) and in CA (n = 68 and n = 65, respectively), and hFetal-CM (n = 70). ns = non-significant; *P < 0.05; **P < 0.01; ***P < 0.001. (For interpretation of the references to colour in this figure legend, the reader is referred to the web version of this article.)

increased sarcomere length in CA compared to BPEL (hESC-CM – BPEL 1.66 ± 0.01 μm, CA 1.83 ± 0.02 μm, P < 0.0001 and hiPS-CM - BPEL 1.68 ± 0.02 μm, CA 1.86 ± 0.01 μm, P < 0.0001) (Fig. 4D). Additionally, and in accordance with contraction stress, both sarcomeric organization and sarcomere length in CA were comparable to that of hFetal-CM (1.82 ± 0.01 μm, P = 0.3976) (Fig. 4B–D).

3.4. Increase in hPSC-CM maturity in vitro

Next, we investigated whether a further increase in cardiomyocyte maturation could be achieved by introducing another step of culture in a T3 thyroid hormone based maturation medium (MM) for 10 additional days (Supplementary Fig. 1). Recent studies have shown that T3 thyroid hormone has the potential to stimulate different characteristics of cardiomyocyte maturation [33]. Both hESC-CMs and hiPS-CMs cultured in MM showed an increase of 140% and 170% in contraction stress, respectively, compared to CMs cultured in BPEL or a 43% and 41% increase compared to CMs in CA media on day 33 (hESC-CM - BPEL 0.21 ± 0.07 mN/mm^2, CA 0.36 ± 0.02 mN/mm^2, MM 0.52 ± 0.04 mN/mm^2 $P < 0.0001$) and (hiPS-CM - BPEL 0.18 ± 0.02 mN/mm^2, CA 0.36 ± 0.02 mN/mm^2, MM 0.51 ± 0.04 mN/mm^2 $P < 0.0001$) (Fig. 5A). Moreover, hPSC-CMs in MM displayed a higher contraction stress than hFetal-CM population (hESC-CM vs hFetal-CM $P = 0.0018$; hiPS-CM vs

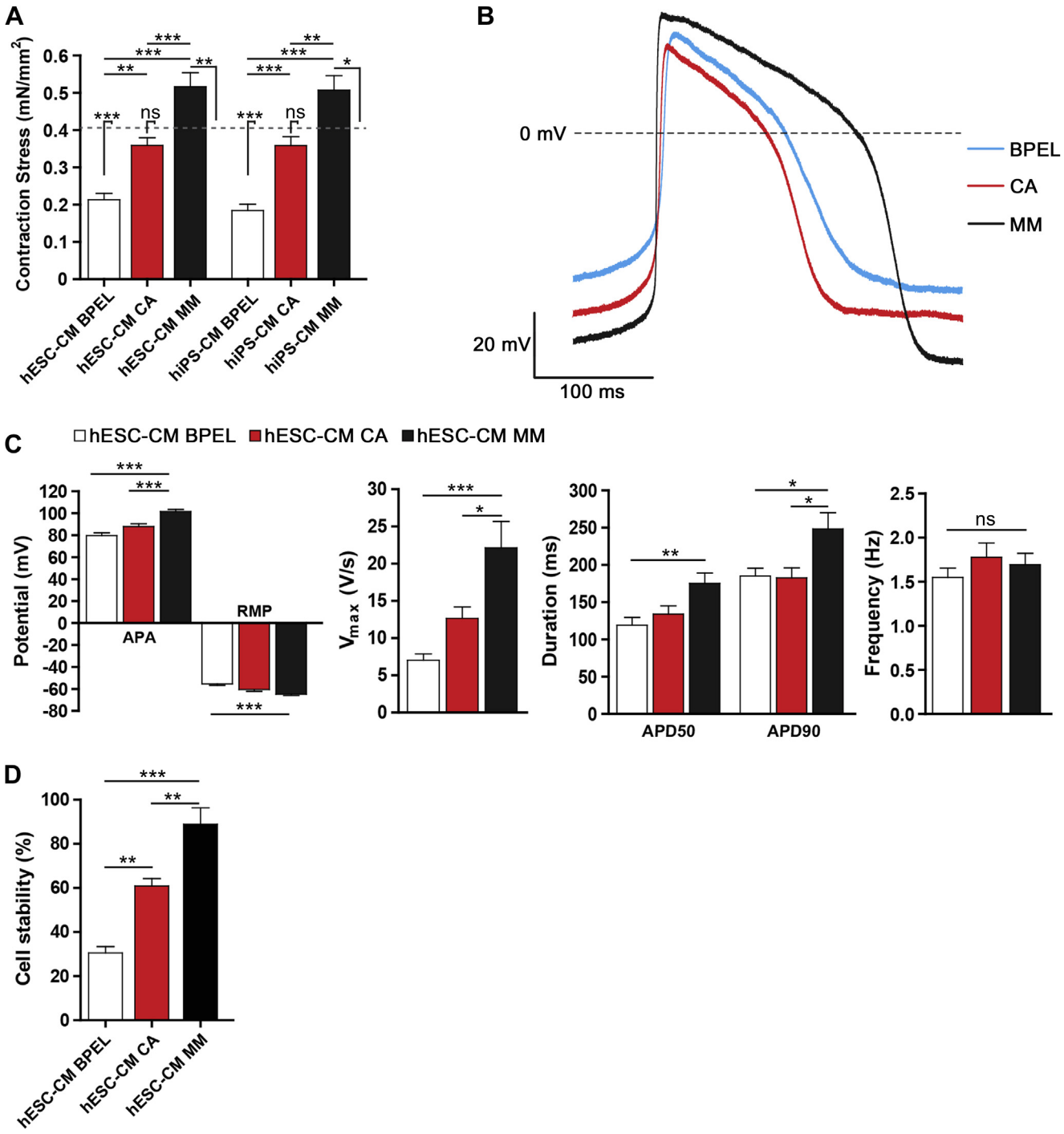

Fig. 5. Increase in hPSC-CM maturation stage *in vitro*. A. Mean contraction stress at day 33 generated by hESC-CM and hiPS-CM in BPEL (n = 40 and n = 46, respectively), in CA (n = 48 and n = 43, respectively) and in MM (n = 46 and n = 46). The dotted line represents the mean contraction stress generated by the hFetal-CM. **B**. Representative examples of spontaneous AP of hESC-CM in the three different media. **C**. Electrophysiological comparison between hESC-CM in BPEL (n = 17), CA (n = 18) and MM (n = 26), with Vmax, RMP, APA, APD50 and APD90 in hESC-CM in MM. **D**. Percentage of stable hESC-CM in CA, BPEL and in MM. ns = non-significant; *P < 0.05; **P < 0.01; ***P < 0.001.

hFetal-CM $P = 0.0084$) (Fig. 5A), indicating that hPSC-CM can be stimulated to mature further in their contractile output *in vitro*, beyond the force level of 2nd trimester human fetal cardiomyocytes. Furthermore, culturing hESC-CM in MM did not increase their cell surface area in comparison with hESC-CMs in CA (hESC-CM in CA 1378 ± 71.95 μm^2 and hESC-CM in MM 1483 ± 90.38 μm^2 $P = 0.36$), while culturing hiPS-CM in MM increased their cell surface area in comparison with hiPS-CM in CA (hiPS-CM in CA 1445 ± 74.39 μm^2 and hiPS-CM in MM 2169 ± 110.2 μm^2 $P < 0.0001$) (Supplementary Fig. 4).

We next examined the electrophysiological maturation state of hESC-CMs in MM by patch-clamp recordings at day 33. The Vmax was significantly increased in hESC-CM in MM in spontaneously beating cells and cells paced at 2 and 3 Hz, whereas hESC-CMs in MM had a lower RMP at all frequencies, indicating electrophysiological maturation. In terms of AP shape, there was an increase in

APA at all tested frequencies, together with an increase in ADP50 and ADP90 (Fig. 5B and C; Supplementary table 3). Furthermore, the number of stable cardiomyocytes capable of generating measurable APs upon medium switch following contraction force measurements increased in MM. Cardiomyocyte stability increased from 29.6% (21 of 71) in BPEL to 60.5% (23 of 38) in CA and to 85.3% (29 of 34) in MM (Fig. 5D).

In order to shed light on possible molecular mechanisms underlying these functional changes we analyzed gene expression on NKX2-5-eGFP sorted hESC-CM. In agreement with functional maturation, a clear increase in expression was observed of genes encoding sarcomeric proteins such as *ACTN2*, *MYBPC3*, *MYH6*, *MYH7*, *TNNI3* and of genes encoding calcium handling proteins like *SERCA2*, *RYR2* and *CACNA1C* in MM cultured cells (Fig. 6A). Contractile maturation is therefore accompanied by upregulation of genes that are important for cardiac contractility, suggesting a causal relationship. Similarly, electrophysiological maturation is likely the result of increased expression of sodium and potassium channel encoding genes such as *SCN5A*, *KCNH2, KCND3, KCNJ12* and *KCNQ1*, with a decrease in *HCN4* (Fig. 6A). Additionally, increased PGC1α expression suggested improvements in bioenergetics, since this gene has been previously shown to regulate mitochondrial biogenesis in these cells [38].

Correspondingly, hPSC-CM in MM displayed improved sarcomeric organization compared with cardiomyocytes in BPEL, although not significantly better than hPSC-CM maintained in CA (Fig. 6B and C). Moreover, hPSC-CM in MM showed increased sarcomere length relative to hPSC-CM in BPEL and CA (hESC-CM – BPEL 1.44 ± 0.05 μm, CA 1.64 ± 0.02 μm, MM 1.85 ± 0.02 μm $P < 0.0001$) and (hiPS-CM - BPEL 1.60 ± 0.02 μm, CA 1.79 ± 0.02 μm, MM 1.98 ± 0.02 μm $P < 0.0001$) (Fig. 6D). Of note, hiPS-CM in MM exhibited better sarcomeric organization and larger sarcomere length than hFetal-CM, indicating a higher level of structural maturation (Fig. 6B–D).

3.5. Cardiomyocyte maturation can be assessed from the direct relationship between contraction force and electrophysiological parameters

Increased contractile force and electrophysiological parameters are important independent indicators of cardiomyocyte maturation. However, little is known about the relationship between the two during cardiomyocyte maturation process. Using the micropatterned polyacrylamide platform we were able to measure contraction force and carry out patch-clamp electrophysiology in the same cells. On day 23, contraction force increase was directly proportional to the increase in APA, APD50 and APD90 (Fig. 7A). However, contraction force did not appear to be correlated with Vmax or RMP at this stage (Fig. 7A). Interestingly, at day 33 the increase of contraction force was strongly correlated with Vmax, RMP and APA but not with APD50 and APD90 (Fig. 7B), indicating that during cardiomyocyte maturation, the different electrophysiological parameters are independently related to contraction force.

4. Discussion

In this study we have shown that cardiomyocytes derived from both hESC and hiPS have comparable contraction stress, but these are lower than those of second trimester hFetal-CM. By adjusting cardiomyocyte culture conditions in a step-wise manner, we were able to increase the contraction stress of single hPSC-CM to values higher than hFetal-CM, indicating cardiomyocyte maturation. Corroborating these findings, we also observed changes in several electrophysiological parameters, sarcomeric organization and gene expression, all of which indicated cardiomyocyte maturation in culture. Interestingly, we observed a strong correlation between electrophysiological and contractile maturation measured in single cells, suggesting involvement of a common pathway for phenotypic and functional cardiomyocyte maturation.

Despite improvement in differentiation methods of hPSC-CM, their relative immaturity limits their possible application in disease modelling, drug discovery, safety pharmacology and regenerative medicine. In order to overcome this hurdle, it is crucial to compare the phenotype and function of hPSC-CM with that of cardiomyocytes from the human heart. Previously, we have shown that hESC-CM and 16 week hFetal-CM were comparable at the electrophysiological level, whereas hESC-CM displayed less defined sarcomeric structures [5]. Others have compared transcriptional levels of cardiac genes of hESC-CM to those of 33–35 weeks fetal heart. However, no direct comparison of contraction stress between hPSC-CM and human primary cardiomyocytes has been made before. So far the contraction stress of 44 ± 11.7 mN/mm^2 measured in adult human papillary muscle strips have been used as a comparison reference value for tissue engineered cardiac patches [12,40]. However, even though 3D engineered tissues have a closer resemblance to the human heart, differences such as cellular composition, ratio of cardiomyocytes versus non-cardiomyocytes, cardiomyocyte orientation, extracellular components and variation in methodology for calculating contractile stress amplitudes [12], cause a considerable variation in the levels of contraction stress output. Although a continuous effort to mimic the human heart in all its complexity is crucial, development of simplified 2D platforms is necessary to complement 3D models, allowing assessment of molecular, phenotypic and functional changes of individual cells without interference from external factors. Our results showed similar contraction stress between hESC-CM and hiPS-CM (0.29 ± 0.01 mN/mm^2 and 0.26 ± 0.01 mN/mm^2, respectively), in agreement with previous reports [13]. These results are comparable to the 0.22 ± 0.07 mN/mm^2 reported for hESC-CM under similar substrate conditions [9]. Moreover, hPSC-CM showed lower contraction stress and sarcomeric organization than 14–19 week hFetal-CM, indicating an earlier maturation stage of these cardiomyocytes under standard culture conditions. Although it has been reported that expression of contractile and remodelling proteins progressed from the first to second trimester [41], not much is known on the functional progression of hFetal-CM during development. Here we have shown that contraction stresses of hFetal-CM are similar from gestation week 14 until 19.

In order to promote hPSC-CM maturation *in vitro* we made use of a commercial defined, nutrient-rich maturation media containing T3 hormone in combination with a more physiologically relevant substrate stiffness and micropatterned adhesive surfaces to standardize the cell shape [16,29]. Cardiomyocyte maturation was determined based on various molecular, phenotypic and functional parameters using combinations of different technologies.

We divided our approach in two steps by analysing hPSC-CM maturation progression at day 23, cultured for 10 days in CA, and at day 33, cultured for an additional 13 days in MM. At day 23, both hESC-CM and hiPS-CM cultured in CA increased their contraction stress by 51% and 66%, respectively, and remarkably achieved a level comparable to that of hFetal-CM. Although this progression in contractility was accompanied by a prolongation of the AP and increased APA amplitude to levels similar to those in human adult ventricular muscle [42], the values for Vmax and RMP, two important parameters of electrophysiological maturation, did not change. Nevertheless, sarcomeric organization and cell size increased, and there was a modest increase in the expression of genes encoding contractile sarcomeric proteins and ion channels. In agreement with these findings, a recent study by Feinberg and colleagues described that improvement in sarcomere organization

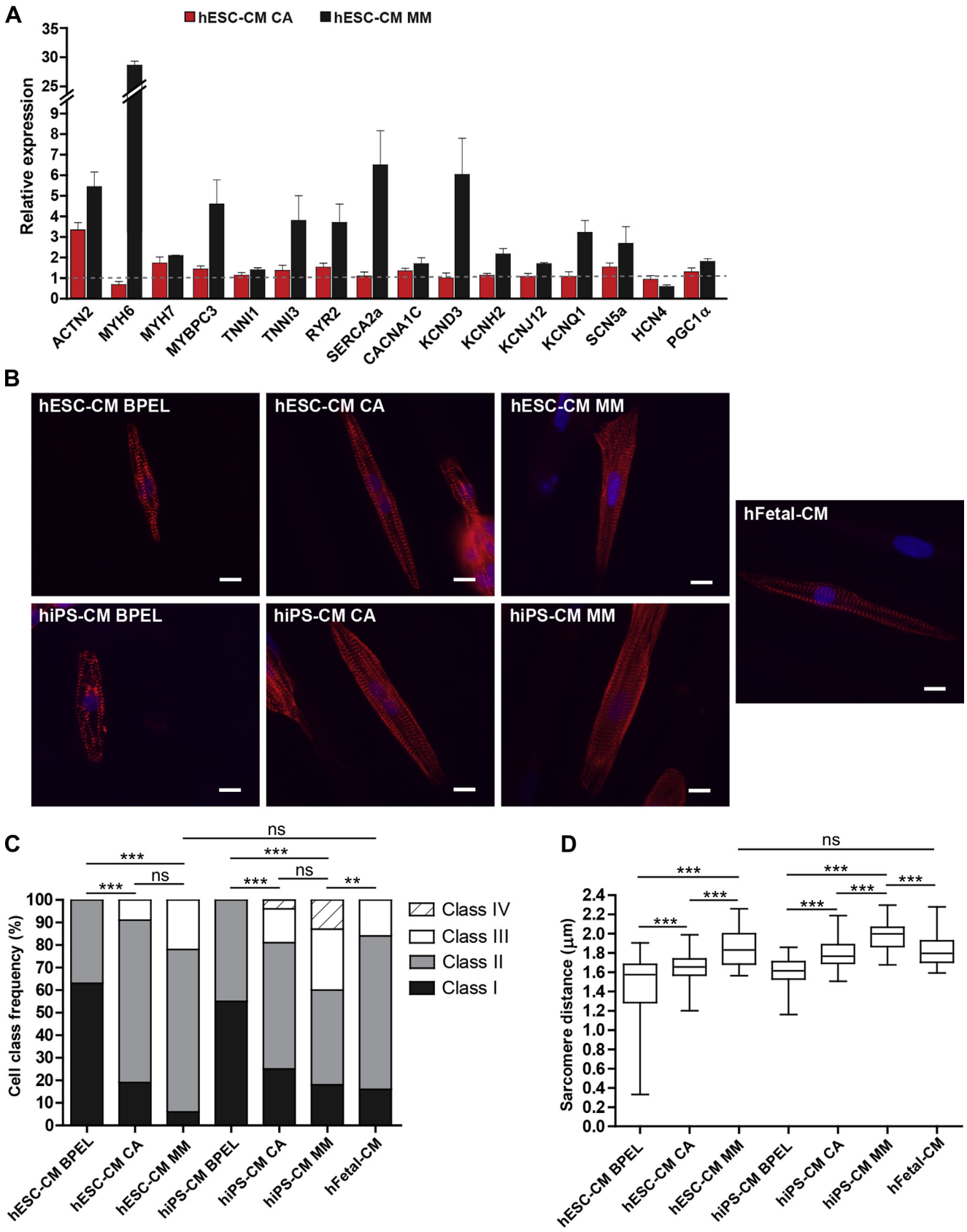

Fig. 6. Changes in gene expression and sarcomeric organization of hPSC-CM in MM. A. Expression of genes encoding: sarcomeric proteins (*ACTN2, MYH6, MHY7, MYBPC3, TNNI1, TNNI3*), calcium handling channels (*RYR2, SERCA2a, CACNA1C*), membrane ion channels (*KCND3, KCNH2, KCNJ12, KCNQ1, SCN5a, HCN4*) and the mitochondrial master regulator PGC1α, normalized to *RPLP* expression. The dotted line represent gene expression levels in hESC-CM in BPEL **B**. Representative images of α-actinin staining (red) and nuclei (blue) of hESC-CM and hiPS-CM in BPEL, in CA and in MM, and of hFetal-CM. Scale bar 10 μm. **C**. Classification of sarcomere organization. HESC-CM and hiPS-CM in BPEL (both n = 74), in CA

led to increased APD, calcium transient kinetics and contraction stress [43], which is consistent with functional maturation. Observed changes in sarcomeric organization and cell size are compatible with the physiological cardiac hypertrophy during development. However, it is worth noting that human adult ventricular myocytes have been reported to have surface areas of 12,315 ± 2103 μm^2 in culture [44], which is approximately 6 fold higher than the average hPSC-CM under these culture conditions.

In the following step we prolonged hPSC-CM culture in a T3-based MM, achieving further cardiomyocyte maturation. hESC-CM and hiPS-CM in MM displayed a higher level of sarcomeric organization and increased their contraction stress by 140% and 170% respectively when compared to CMs cultured in BPEL and by 43% and 41% in comparison to CMs in CA. These results are in accordance with previously reported findings that T3 hormone increased contractile maturation in hiPS-CM [33]. Interestingly, both hESC-CM and hiPS-CM in MM generated significantly higher contraction stress than hFetal-CM. In agreement with increased contractility, gene expression analysis revealed increased expression of genes encoding contractile sarcomeric proteins such as *ACTN2, MYBPC3, MYH6, MYH7* and *TNNI3*, which have all been described to have lower expression in hESC-CM than in human adult heart [45]. In particular the β-myosin heavy chain (*MYH7*) and troponin I type 3 (*TNNI3*) are major isoforms in the adult heart [46,47] and their increase in expression has been previously linked to cardiomyocyte maturation [8]. Although the α-myosin heavy chain (*MYH6*) isoform is not the dominant MHC isoform in the adult human heart, its expression in adult human cardiomyocytes is higher than in hESC-CM [45]. Therefore, the nearly 30-fold upregulation of α-myosin heavy chain expression in hESC-CM in MM, is likely associated with cardiomyocyte maturation.

Progression in maturation was not only found in contraction but was also observed electrophysiologically. hESC-CM cultured in MM on polyacrylamide gels displayed overall improvements in electrophysiological maturation with a significant increase in the Vmax, APA, APD50, APD90 and a decrease in RMP at all tested frequencies. Although the AP amplitude, APD50 and APD90 of hESC-CM on MM reached levels similar to human adult ventricular myocytes [42], the levels of Vmax and RMP were still relatively low in comparison with the adult situation. Therefore, additional maturation steps are still required to reach levels in adult cardiomyocytes. Maintaining cardiomyocyte cultures for a prolonged time in MM may be sufficient to accomplish such goal, since a recent study described Vmax of 188.7 ± 12.6 V/s and RMP of −68.2 ± 2.1 mV in hESC-CM by culturing for ≤120 days [14].

In accordance with the functional improvements, hESC-CMs maintained in MM showed increased expression of distinct cardiac ion channel genes. In particular, *KCNJ12* encoding the primary subunit of the inwardly rectifying potassium channel that contributes to $I_{K1,}$ the current responsible for lowering the RMP, was increased. Furthermore, the RMP itself influences the availability of the other ion channels in the membrane. Increased expression of the *SCN5A* gene encoding the alpha-subunit of the sodium channel conducting I_{Na}, together with a lower RMP, are responsible for the increase in the Vmax. Increased expression of *KCND3*, encoding a potassium voltage-gated channel conducting the transient outward potassium current (I_{to1}), promotes a more mature AP shape [48]. The *KCNH2* and *KCNQ1* genes encode the alpha-subunits of potassium channels responsible for the rapid and slow delayed rectifier potassium currents (I_{kr} and I_{Ks}, respectively), therefore an increase in their expression advocates a faster repolarization of the cell membrane which can be linked to shorter AP duration. However, the APD_{50} and APD_{90} were prolonged in the hESC-CMs in MM, which may be explained by the increase in the availability of the L-type voltage-dependent calcium channel (where *CACNA1C* encodes the α-subunit), which is responsible for the inward flow of calcium and consequent membrane depolarization [49]. The net result is in agreement with electrophysiological maturation, since it has been shown previously that the expression of genes encoding ion channels is low in hESC-CM when compared to that in adult heart [4]. Furthermore, the funny current (I_f) channel HCN4, which delineates the cardiac conduction system and is important for pacemaking activity [50], is also expressed in early immature cardiomyocytes during embryonic development but not expressed in adult atrial or ventricular cardiomyocytes. Therefore, *HCN4* downregulation in MM is also consistent with phenotypic maturation of cardiomyocytes of working myocardium. Furthermore, increased expression of genes responsible for calcium handling and metabolism was also observed, suggesting functional maturation of the calcium kinetics and metabolism. In summary, hESC-CM in MM displayed increased expression of genes responsible for contraction, calcium handling, electrophysiology and metabolism, all indicating a more advanced stage of cardiomyocyte maturation. These effects can at least partially be attributed to T3, since this has been described as directly inducing *MYH6*, *SERCA2*, *KCND3* and *PGC1α* expression [31,51]. Each of these genes has a critical role in each functional component characteristic of cardiomyocytes, and their upregulation may influence the overall maturation. Furthermore, single cell stability increased significantly in MM compared to BPEL and CA; this could also be attributed to overall cardiomyocyte maturation. In accordance with the contractility, electrophysiological and gene expression maturation, the sarcomeric organization of hPSC-CM in MM improved significantly in comparison to hPSC-CM in BPEL. Corroborating this observation hPSC-CM, displayed a stepwise increase in sarcomere length from BPEL to CA and to MM, reaching lengths similar to those observed in 3D tissue patches [12]. Interestingly, at this stage hiPSC-CM displayed better sarcomeric organization, with highly organized sarcomeres filling more than 90% of the cell, and greater sarcomere lengths than hESC-CM. This difference is perhaps attributable to inherent differences between the cells lines. Additionally, hiPSC-CM show significantly increased sarcomeric organization in comparison to the hFetal-CM, demonstrating a more mature structure.

Altogether, these improvements in cardiomyocyte contractility, electrophysiology, sarcomere organization and gene expression are indicative of an overall increase in the hPSC-CM maturation stage. These parameters together can be considered adequate reporters of maturation. Interestingly, this 2D platform allowed the measurement of contraction forces and electrophysiology of individual cells in different maturation stages, enabling us to determine the relationship between these two key characteristics during cardiomyocyte maturation. We observed that the increase in contraction force is only correlated with the increase in APD50, APD90 and APA on day 23, while on day 33 there was also a correlation between Vmax, APA and RMP. Since CA does not induce progression in hESC-CM Vmax and RMP, there is no correlation between these parameters and the CA induced increase in contraction force. In MM, however, the biochemical cue from T3 promoted improvement in Vmax and RMP together with an improvement in contraction force. One possible explanation for these observations could be that changes in the electrophysiological parameters to a mature phenotype occur in a process-dependent fashion with parameters such as Vmax, APA and RMP

(n = 47 and n = 45, respectively) and in MM (n = 46 and n = 46, respectively), and hFetal-CM (n = 76). **D**. Median, maximum and minimum sarcomere lengths of hESC-CM and hiPS-CM in BPEL (n = 38 and n = 34, respectively), in CA (n = 42 and n = 44, respectively) and in MM (n = 40 and n = 43, respectively), and hFetal-CM (n = 70). ns = non-significant; **P < 0.01; ***P < 0.001. (For interpretation of the references to colour in this figure legend, the reader is referred to the web version of this article.)

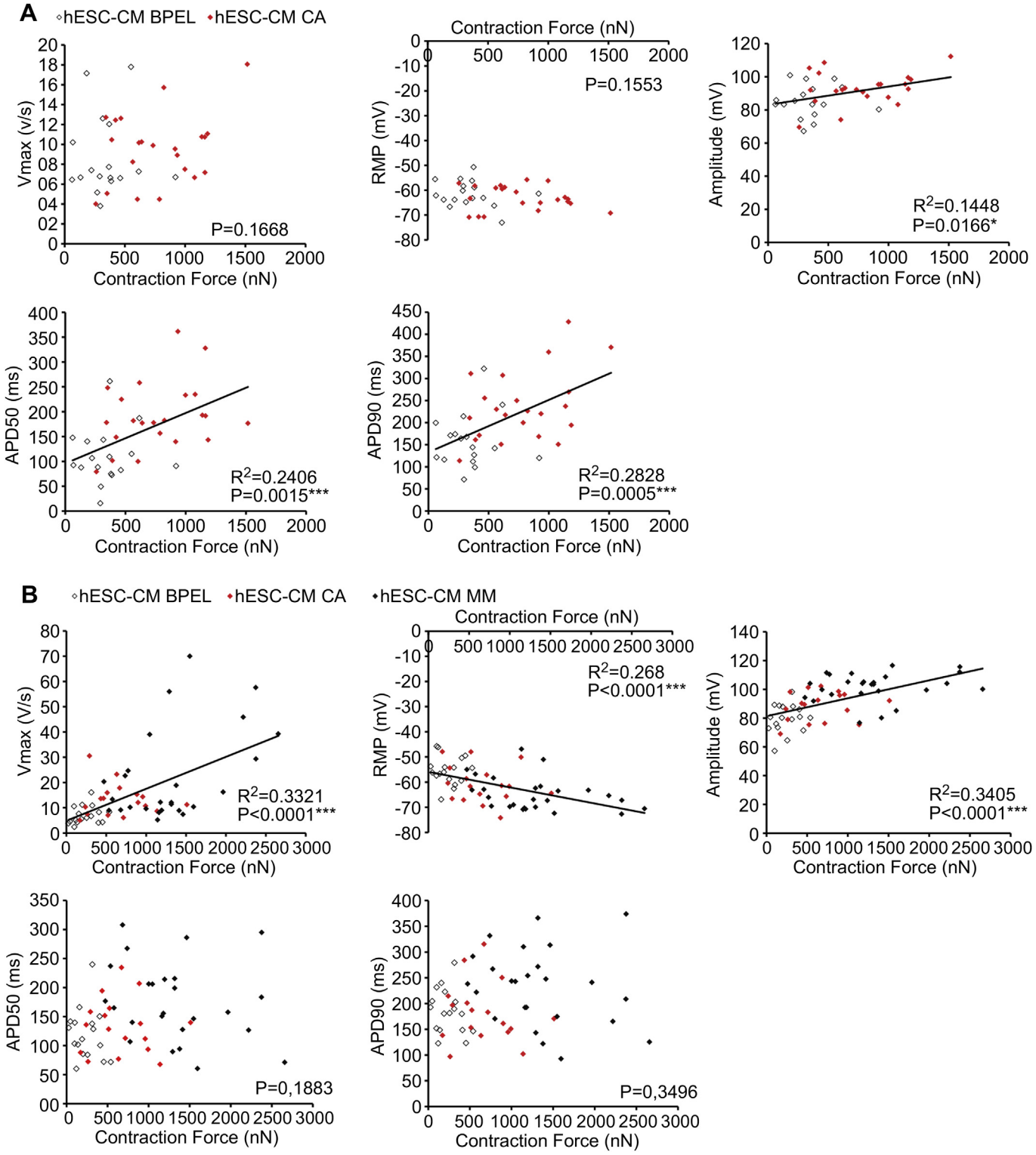

Fig. 7. Relationship between different electrophysiology parameters and contraction force during cardiomyocyte maturation. **A.** Relation between contraction force (nN) and Vmax, RMP, APA, APD50 and APD90 in single hESC-CM at day 23 (n = 42 including hESC-CM in BPEL (white) and in CA (red)). **B**. Relation between contraction force (nN) and Vmax, RMP, APA, APD50 and APD90 on single hESC-CM at day 33 (n = 60 including hESC-CM in BPEL (white), in CA (red) and in MM (black)). The P values refer to significance in correlation between the two parameters. With $P > 0.05$ no correlation was considered existent and therefore no linear regression line was drawn; With $P < 0.05^{*}$ and $P < 0.01^{**}$ a correlation was considered existent and a linear regression line was drawn (black line) with the respective R^2. With $P < 0.0001^{***}$ a strong correlation was considered existent and a linear regression line was drawn (black line) with the respective R^2. (For interpretation of the references to colour in this figure legend, the reader is referred to the web version of this article.)

as late-stage alterations. Alternatively, the lack of significant correlation of these electrophysiological parameters and contractility at day 23 in CA medium may suggest independent mechanisms of maturation at this stage. The presence of T3 in the late stage of maturation (MM) may directly affect regulation of genes encoding for sarcomeric and ion channels, suggesting a possible common pathway responsible for the synchronous progression of both electrophysiological parameters and contraction force. In this regard, it is of interest to note that T3 has been shown to increase the inward rectifying potassium I_{k1} currents in guinea pig ventricular myocytes [52], which has a prominent effect on RMP (and Vmax), but also on shortening of APDs. These results indicate that different electrophysiological parameters correlate with the contractile force machinery in a distinct manner during maturation, which may be dependent on the stage or mechanism of maturation.

5. Conclusions

This is the first study directly comparing contraction stress generation between single hPSC-CM and single hFetal-CM on substrates with the same stiffness, establishing the contractile maturation level of hPSC-CM relative to a human fetal stage. Additionally, here we showed increased hPSC-CM maturation *in vitro,* with increased contractile force, electrophysiological maturation, improved sarcomeric organization and increased expression of cardiac-specific genes. During this progression in maturation we established a correlation between contraction and electrophysiology. This improvement in cardiomyocyte phenotype is important for advancing applications of hPSC-CM in cardiac disease modelling, drug discovery and development and regenerative medicine.

Disclosure statement

Robert Passier and Christine Mummery are co-founders of Pluriomics BV.

Sources of funding

The project was supported by The Netherlands Organization for Scientific Research (NWO-FOM) within the program on Mechanosensing and Mechanotransduction by Cells (FOM 09MMC02) (MCR, RP, CLM), the Marie Curie COFUND programme “U-Mobility” co-financed by Universidad de Malaga and the European Community's Seventh Framework Programme under Grant Agreement No.246550 (JAG), the Rembrandt Institute (GK), European Research Council (ERCAdG 323182 to CLM) and the Netherlands Institute of Regenerative Medicine (LT, MB, C d'A).

Acknowledgments

The authors are grateful to Prof. Micah Dembo, Boston University, for providing the LIBTRC program package for computing traction forces and to Stephanie S. Chang for training on the traction force technique. The authors would also like to thank Matthew Birket and Dorien Ward-van Oostwaard for their technical support with cell culture.

Appendix A. Supplementary data

Supplementary data related to this article can be found at http://dx.doi.org/10.1016/j.biomaterials.2015.01.067.

References

[1] Mummery CL, Zhang J, Ng ES, Elliott D a, Elefanty AG, Kamp TJ. Differentiation of human embryonic stem cells and induced pluripotent stem cells to cardiomyocytes: a methods overview. Circ Res 2012;111(3):344–58.
[2] Bellin M, Marchetto MC, Gage FH, Mummery CL. Induced pluripotent stem cells: the new patient? Nat Rev Mol Cell Biol Nat Publ Group 2012;13(11):713–26.
[3] Davis RP, van den Berg CW, Casini S, Braam SR, Mummery CL. Pluripotent stem cell models of cardiac disease and their implication for drug discovery and development. Trends Mol Med 2011;17(9):475–84. Elsevier Ltd.
[4] Synnergren J, Améen C, Jansson A, Sartipy P. Global transcriptional profiling reveals similarities and differences between human stem cell-derived cardiomyocyte clusters and heart tissue. Physiol Genomics 2012;44(4):245–58.
[5] Mummery C, Ward-van Oostwaard D, Doevendans P, Spijker R, van den Brink S, Hassink R, et al. Differentiation of human embryonic stem cells to cardiomyocytes: role of coculture with visceral endoderm-like cells. Circulation 2003;107(21):2733–40.
[6] Lopaschuk GD, Jaswal JS. Energy metabolic phenotype of the cardiomyocyte during development, differentiation, and postnatal maturation. J Cardiovasc Pharmacol 2010;56(2):130–40.
[7] Maillet M, van Berlo JH, Molkentin JD. Molecular basis of physiological heart growth: fundamental concepts and new players. Nat Rev Mol Cell Biol 2013;14(1):38–48. Nature Publishing Group.
[8] Yang X, Pabon L, Murry CE. Engineering adolescence: maturation of human pluripotent stem cell-derived cardiomyocytes. Circ Res 2014;114(3):511–23.
[9] Kita-Matsuo H, Barcova M, Prigozhina N, Salomonis N, Wei K, Jacot JG, et al. Lentiviral vectors and protocols for creation of stable hESC lines for fluorescent tracking and drug resistance selection of cardiomyocytes. PLoS One 2009;4(4):e5046.
[10] Stoehr A, Neuber C, Baldauf C, Vollert I, Friedrich FW, Flenner F, et al. Automated analysis of contractile force and Ca2+ transients in engineered heart tissue. Am J Physiol Heart Circ Physiol 2014;306(9):H1353–63.
[11] Kensah G, Roa Lara A, Dahlmann J, Zweigerdt R, Schwanke K, Hegermann J, et al. Murine and human pluripotent stem cell-derived cardiac bodies form contractile myocardial tissue in vitro. Eur Heart J 2013;34(15):1134–46.
[12] Zhang D, Shadrin IY, Lam J, Xian H-Q, Snodgrass HR, Bursac N. Tissue-engineered cardiac patch for advanced functional maturation of human ESC-derived cardiomyocytes. Biomaterials 2013;34(23):5813–20. Elsevier Ltd.
[13] Hazeltine LB, Simmons CS, Salick MR, Lian X, Badur MG, Han W, et al. Effects of substrate mechanics on contractility of cardiomyocytes generated from human pluripotent stem cells. Int J Cell Biol 2012;2012:508294.
[14] Lundy SD, Zhu W-Z, Regnier M, Laflamme M a. Structural and functional maturation of cardiomyocytes derived from human pluripotent stem cells. Stem Cells Dev 2013;22(14):1991–2002.
[15] Jacot JG, McCulloch AD, Omens JH. Substrate stiffness affects the functional maturation of neonatal rat ventricular myocytes. Biophys J 2008;95(7):3479–87.
[16] Kuo P-L, Lee H, Bray M-A, Geisse N a, Huang Y-T, Adams WJ, et al. Myocyte shape regulates lateral registry of sarcomeres and contractility. Am J Pathol 2012;181(6):2030–7. Elsevier Inc.
[17] Gerdes a M, Kellerman SE, Moore J a, Muffly KE, Clark LC, Reaves PY, et al. Structural remodeling of cardiac myocytes in patients with ischemic cardiomyopathy. Circulation 1992;86(2):426–30.
[18] Xia Yang, Maximilian Buja L, Scarpulla Richard C, JBM. Electrical stimulation of neonatal cardiomyocytes results in the sequential activation of nuclear genes governing mitochondrial. Proc Natl Acad Sci 1997;94:11399–404 (October).
[19] Mihic A, Li J, Miyagi Y, Gagliardi M, Li S-H, Zu J, et al. The effect of cyclic stretch on maturation and 3D tissue formation of human embryonic stem cell-derived cardiomyocytes. Biomaterials 2014;35(9):2798–808. Elsevier Ltd.
[20] Kim C, Wong J, Wen J, Wang S, Wang C, Spiering S, et al. Studying arrhythmogenic right ventricular dysplasia with patient-specific iPSCs. Nature 2013;494(7435):105–10. Nature Publishing Group.
[21] Snir M, Kehat I, Gepstein A, Coleman R, Itskovitz-Eldor J, Livne E, et al. Assessment of the ultrastructural and proliferative properties of human embryonic stem cell-derived cardiomyocytes. Am J Physiol Heart Circ Physiol 2003;285(6):H2355–63.
[22] Kadota S, Minami I, Morone N, Heuser JE, Agladze K, Nakatsuji N. Development of a reentrant arrhythmia model in human pluripotent stem cell-derived cardiac cell sheets. Eur Heart J 2013;34(15):1147–56.
[23] Chopra A, Tabdanov E, Patel H, Janmey P a, Kresh JY. Cardiac myocyte remodeling mediated by N-cadherin-dependent mechanosensing. Am J Physiol Heart Circ Physiol 2011;300(4):H1252–66.
[24] McCain ML, Parker KK. Mechanotransduction: the role of mechanical stress, myocyte shape, and cytoskeletal architecture on cardiac function. Pflugers Arch 2011;462(1):89–104.
[25] Pijnappels D a, Schalij MJ, Ramkisoensing A a, van Tuyn J, de Vries A a F, van der Laarse A, et al. Forced alignment of mesenchymal stem cells undergoing cardiomyogenic differentiation affects functional integration with cardiomyocyte cultures. Circ Res 2008;103(2):167–76.
[26] Kléber AG, Rudy Y. Basic mechanisms of cardiac impulse propagation and associated arrhythmias. Physiol Rev 2004;84(2):431–88.
[27] Walsh KB, Parks GE. Changes in cardiac myocyte morphology alter the properties of voltage-gated ion channels. Cardiovasc Res 2002;55(1):64–75.

[28] Feinberg AW, Feigel A, Shevkoplyas SS, Sheehy S, Whitesides GM, Parker KK. Muscular thin films for building actuators and powering devices. Science 2007;317(5843):1366–70.
[29] Bray M-A, Sheehy SP, Parker KK. Sarcomere alignment is regulated by myocyte shape. Cell Motil Cytoskelet 2008;65(8):641–51.
[30] Pascual A, Aranda A. Thyroid hormone receptors, cell growth and differentiation. Biochim Biophys Acta 2013;1830(7):3908–16. Elsevier B.V.
[31] Klein I, Danzi S. Thyroid disease and the heart. Circulation 2007;116(15):1725–35.
[32] Lee Y-K, Ng K-M, Chan Y-C, Lai W-H, Au K-W, Ho C-YJ, et al. Triiodothyronine promotes cardiac differentiation and maturation of embryonic stem cells via the classical genomic pathway. Mol Endocrinol 2010;24(9):1728–36.
[33] Yang X, Rodriguez M, Pabon L, Fischer K a, Reinecke H, Regnier M, et al. Triiodo-l-thyronine promotes the maturation of human cardiomyocytes-derived from induced pluripotent stem cells. J Mol Cell Cardiol 2014;72:296–304. Elsevier Ltd.
[34] Elliott D a, Braam SR, Koutsis K, Ng ES, Jenny R, Lagerqvist EL, et al. NKX2-5(eGFP/w) hESCs for isolation of human cardiac progenitors and cardiomyocytes. Nat Methods 2011;8(12):1037–40.
[35] Ng ES, Davis R, Stanley EG, Elefanty AG. A protocol describing the use of a recombinant protein-based, animal product-free medium (APEL) for human embryonic stem cell differentiation as spin embryoid bodies. Nat Protoc 2008;3(5):768–76.
[36] Rape AD, Guo W-H, Wang Y-L. The regulation of traction force in relation to cell shape and focal adhesions. Biomaterials 2011;32(8):2043–51. Elsevier Ltd.
[37] Frey MT, Engler A, Discher DE, Lee J, Wang Y-L. Microscopic methods for measuring the elasticity of gel substrates for cell culture: microspheres, microindenters, and atomic force microscopy. Methods Cell Biol 2007;83(07):47–65.
[38] Birket MJ, Casini S, Kosmidis G, Elliott D a, Gerencser A a, Baartscheer A, et al. PGC-1α and reactive oxygen species regulate human embryonic stem cell-derived cardiomyocyte function. Stem Cell Reports 2013;1(6):560–74. The Authors.
[39] Claire Robertson SCG. Maturation phases of human pluripotent stem cell-derived cardiomyocytes. Stem Cells 2013;31(5):1–17.
[40] Hasenfuss G, Mulieri L a, Blanchard EM, Holubarsch C, Leavitt BJ, Ittleman F, et al. Energetics of isometric force development in control and volume-overload human myocardium. Comparison with animal species. Circ Res 1991;68(3):836–46.
[41] Iruretagoyena JI, Davis W, Bird C, Olsen J, Radue R, Teo Broman a, et al. Metabolic gene profile in early human fetal heart development. Mol Hum Reprod 2014;20(7):690–700.
[42] Koncz I, Szél T, Bitay M, Cerbai E, Jaeger K, Fülöp F, et al. Electrophysiological effects of ivabradine in dog and human cardiac preparations: potential anti-arrhythmic actions. Eur J Pharmacol 2011;668(3):419–26. Elsevier B.V.
[43] Feinberg AW, Alford PW, Jin H, Ripplinger CM, Werdich A a, Sheehy SP, et al. Controlling the contractile strength of engineered cardiac muscle by hierarchal tissue architecture. Biomaterials 2012;33(23):5732–41. Elsevier Ltd.
[44] Li RK, Mickle D a, Weisel RD, Carson S, Omar S a, Tumiati LC, et al. Human pediatric and adult ventricular cardiomyocytes in culture: assessment of phenotypic changes with passaging. Cardiovasc Res 1996;32(2):362–73.
[45] Xu XQ, Soo SY, Sun W, Zweigerdt R. Global expression profile of highly enriched cardiomyocytes derived from human embryonic stem cells. Stem Cells 2009;27(9):2163–74.
[46] Gorza L, Mercadier JJ, Schwartz K, Thornell LE, Sartore S, Schiaffino S. Myosin types in the human heart. An immunofluorescence study of normal and hypertrophied atrial and ventricular myocardium. Circ Res 1984;54(6):694–702.
[47] Saggin L, Gorza L, Ausoni S, Schiaffino S. Troponin I switching in the developing heart. J Biol Chem 1989;264(27):16299–302.
[48] Adriana Blazeski LT. Cardiomyocytes derived from human induced pluripotent stem cells as models for normal and diseased cardiac electrophysiology and contractility. Prog Biophys Mol Biol 2012;110(0):166–77.
[49] Kim C, Majdi M, Xia P, Wei K a, Talantova M, Spiering S, et al. Non-cardiomyocytes influence the electrophysiological maturation of human embryonic stem cell-derived cardiomyocytes during differentiation. Stem Cells Dev 2010;19(6):783–95.
[50] Accili E a, Proenza C, Baruscotti M, DiFrancesco D. From funny current to HCN channels: 20 years of excitation. News Physiol Sci 2002;17(6):32–7.
[51] Weitzel JM, Radtke C, Seitz HJ. Two thyroid hormone-mediated gene expression patterns in vivo identified by cDNA expression arrays in rat. Nucleic Acids Res 2001;29(24):5148–55.
[52] Sakaguchi Y, Cui G, Sen L. Acute effects of thyroid hormone on inward rectifier potassium channel currents in Guinea pig ventricular myocytes. Endocrinology 1996;137(11):4744–51.